

STAFF SUMMARY SHEET

	TO	ACTION	SIGNATURE (Surname), GRADE AND DATE		TO	ACTION	SIGNATURE (Surname), GRADE AND DATE
1	DFP	sig	<i>[Signature]</i> 27 Feb 2013	6			
2	DFER	approve	<i>[Signature]</i> 27 Feb 2013	7			<i>[Signature]</i>
3	DFP	action		8			
4				9			
5				10			

SURNAME OF ACTION OFFICER AND GRADE	SYMBOL	PHONE	TYPIST'S INITIALS	SUSPENSE DATE
Asmolova, CIV	DFP	333-7646	oa	20130405
SUBJECT Clearance for Material for Public Release				DATE
USAFA-DF-PA- 273				20130325

SUMMARY

- PURPOSE.** To provide security and policy review on the document at Tab 1 prior to release to the public.
- BACKGROUND.**
Authors: Olha Asmolova, Geoff Andersen, Michael E. Dearborn, Matthew G. McHarg, Trey Quiller and Thomas Murphey
Title: Optical analysis of a membrane photon sieve space telescope
Document type: Article
Description: Proceedings paper for SPIE Conference on Defense Security and Sensing, Baltimore, MA, 28 April-3 May 2013.
Release Information: This material does not contain any ITAR restricted details
Previous Clearance information: None
Recommended Distribution Statement: Distribution A, Approved for public release, distribution unlimited.
- DISCUSSION.** This research is funded by DARPA but conducted at USAFA. USAFA public release is required.
- VIEWS OF OTHERS.** None
- RECOMMENDATION.** Sign coord block above indicating document is suitable for public release. Suitability is based solely on the document being unclassified, not jeopardizing DoD interests, and accurately portraying official policy.

// signed //

CORY T. LANE, Maj, USAF
Director of Research
Department of Physics

Tabs

- Article for SPIE DSS conference

Asmolova
13014

Optical analysis of a membrane photon sieve space telescope

Olha Asmolova^a, Geoff Andersen^a, Michael E. Dearborn^a, Matthew G. McHarg^a, Trey Quiller^a
Thomas Murphey^b

^aHQ USAFA/DFP, 2354 Fairchild Dr., Ste 2A31, USAF Academy, CO 80840

^bAir Force Research Laboratory/RVSV, Aberdeen Ave. SE, Kirtland, NM 87117

ABSTRACT

This paper focuses on recent progress in designing FalconSAT-7, a 3U CubeSat solar telescope designed to image the Sun from low Earth orbit. The telescope system includes a deployable structure that supports a membrane photon sieve under tension as well as secondary optics. To satisfy mission requirements to demonstrate diffraction limited imaging capability of this collapsible, $f/2$ diffractive primary we have completed studying a number of effects on membrane material that can affect system imaging quality.

Keywords: Space telescopes, lightweight optics, diffractive optics

1. INTRODUCTION

We are designing a space telescope with a deployable membrane primary¹⁻⁴ to image the Sun at H-alpha wavelengths. The primary optic is an $F/2$, 0.2 m diameter photon sieve - a diffractive element consisting of billions of tiny circular pads on a transparent zero-CTE polyimide substrate with a mass less than 2 grams. Aside from being lightweight and compactable, the use of flat optics greatly reduces the mechanical engineering constraints over conventional reflective elements. When deployed in a low Earth orbit the membrane is pulled taut by a triangular pantograph support structure and the telescope will collect images of the Sun for transmission to a ground station at the U.S. Air Force Academy.

2. FALCONSAT-7

FalconSAT-7 is a student mission to demonstrate a solar space telescope incorporating a membrane photon sieve deployed from a 3U CubeSat (dimensions 0.3m×0.1m×0.1m). Half of this volume is devoted to avionics, including pointing control, communications, power and associated electronics. Within the remaining volume we have configured the payload (called Peregrine) which consists of the membrane, deployment structure, secondary optics (including secondary lenses, baffles, filter and fold mirrors) and two cameras (Fig.1).

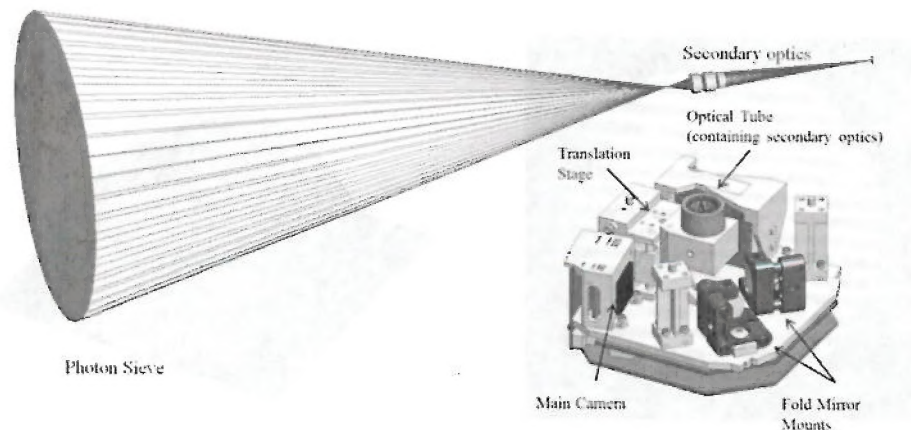


Figure 1. A schematic of the optical system based on our Zemax model (left) and CAD model (right) of the optical platform prototype containing the main camera, translation stage, fold mirrors, and secondary optics.

Peregrine is designed to observe the sun from a low-Earth orbit at a wavelength of 656.45nm (H-alpha). This wavelength was chosen to ensure that even with a narrow bandwidth and low efficiency there would be sufficient photon flux to obtain images under the most modest of operating conditions.

3. MEMBRANE PRIMARY

A photon sieve is a Fresnel zone plate (FZP) in which the rings have been broken up into many individual circular holes. For an infinite conjugate, binary FZP of focal length (f) at a wavelength (λ), the radial distance to the center of the n th bright zone is given by (r_n):

$$r_n^2 = 2nf\lambda + n^2\lambda^2 \quad (1)$$

The width (w) of each zone is

$$w = \frac{\lambda f}{2r_n} \quad (2)$$

Photon sieve for the Peregrine telescope was generated using MatLab code, resulting in 53 GB of data. The data were organized in GBR format file that contains x and y coordinates for each hole and its diameter. For the H-alpha wavelength 20 cm the photon sieve master has just over 19 thousand rings with approximately 2.5 billion holes total. The GBR file was converted to GDS and a rigid photon sieve master was constructed on chrome coated quartz using electron beam photolithography.

A membrane photon sieve was then created in a near zero coefficient of thermal expansion (CTE), 20 micron thick Novastrat polyimide (manufactured by Nexolve) by contact printing of the rigid master. Diffractive membrane primaries have many advantages including mass, volume and fabrication, but there are two trade-offs; decreased efficiency and large dispersion⁵⁻⁷. In the case of Peregrine, the useful bandwidth is only 9 pm.

4. EXPERIMENTAL RESULTS

4.1 Photon sieve master analysis

In order to test the photon sieve, we constructed a high quality 150mm diameter reference beam. Light focused by the photon sieve master was recollimated with a high quality camera lens and made to interfere with an aberration-free reference beam. The resulting interferogram showed near diffraction limited performance with only a very small amount of coma and astigmatism present due to glass imperfections.

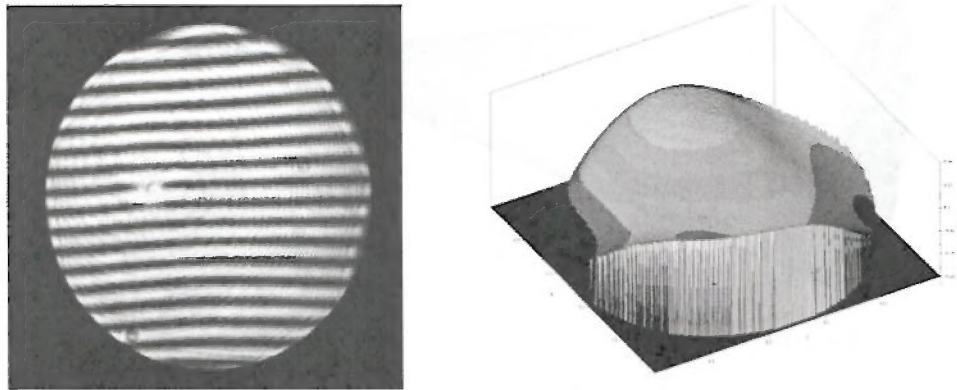


Figure 2. An interferogram of the focused wavefront (left) and its surface map (right). Analysis showed diffraction limited performance with an RMS error of 0.096 waves (0.47 waves PV) with 0.03 waves of spherical aberration.

4.2 Optical system resolution test

In the test set-up described above, the Peregrine telescope produced a focal spot with a diameter of $16.2\text{ }\mu\text{m}$ (Fig. 3) as expected from theoretical calculations and Zemax modeling.

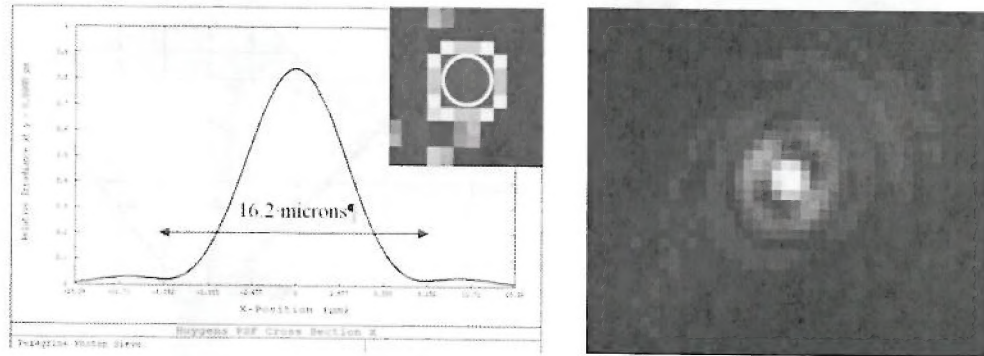


Figure 3. The modeled point spread function cross section in Zemax (left) and the actual PSF captured (right).

The spatial filter was replaced with a 1951 USAF resolution test chart. An image of the chart produced by Peregrine is also shown in Fig. 4. It was possible to resolve 144 lp/mm, which is the diffraction limit.

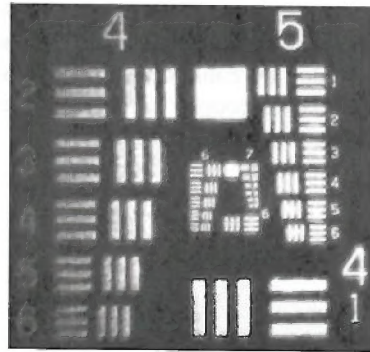


Figure 4. An image of the resolution test chart produced by the photon sieve

4.3 Opto-mechanical analysis

The deployment structure of FalconSAT-7 consists of three spring-load pantographs stowed under compression and a catenary-shaped membrane gently folded inside the center. Once in orbit, the hinged end panel opens by the release of a burn wire and the pantographs deploy automatically. The membrane is pulled flat by tension in the pantographs and lanyards that run the full length to the spacecraft bus. A small, secondary inspection camera set in the top corner of the CubeSat will be used to observe the membrane deployment.

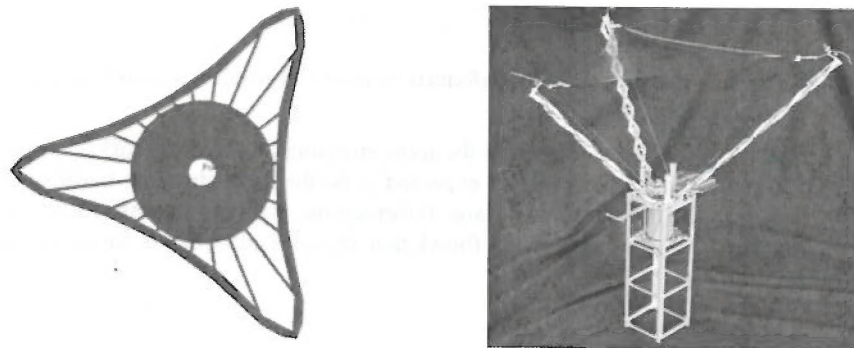


Figure 5. The photon sieve is patterned on the circular region in the center of the flat triangular membrane supported by pantographs and lanyards.

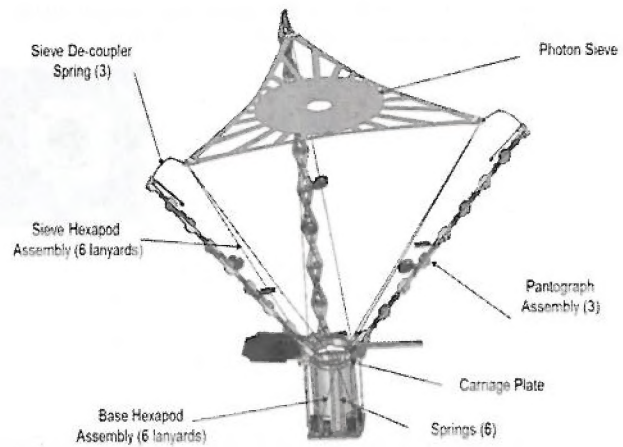
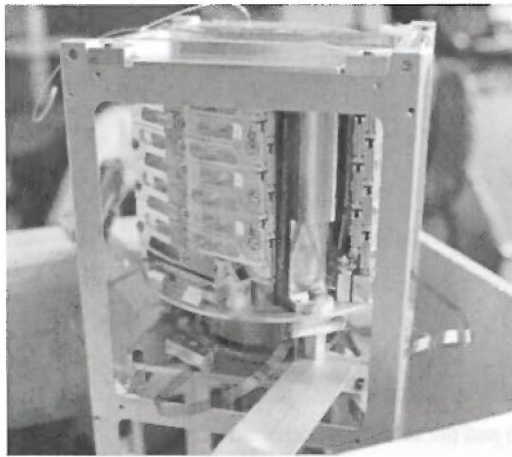


Figure 6. The membrane photon sieve stowed (left) and deployed (right) with the double hexapod support structure. The photon sieve is folded and stored in a cylinder that is 6 cm in diameter and 10 cm tall. The cylinder is anchored to the deployment structure baseplate and located inside the three stowed pantographs.

We completed an opto-mechanical modeling cycle to determine optical imaging performance. The elastic deformations of the photon sieve were analyzed in a finite element model that included the photon sieve, connectors to the photon sieve, lanyards and de-coupler springs. From this model, we could determine the in-plane and out-of-plane deformations of the photon sieve due to variations of the tips of the de-coupler springs and then further analyze the effect of these deformations in Zemax⁸. A typical result of this analysis is shown in Figure 7.

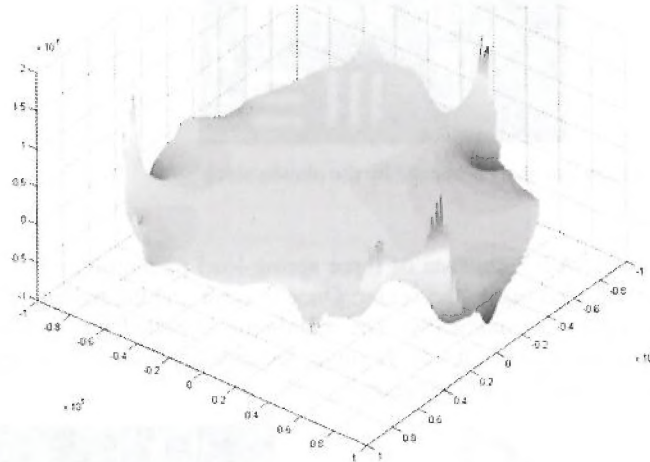


Figure 7. A surface plot of the out-of-plane membrane deformations due to off-nominal positioning of the de-coupling springs. The full vertical scale is 3 microns.

Figure 8 shows an image produced by photon sieve for the most stressing deployment (off nominal case), when the tips of the de-coupling springs are misaligned. This case is expected to be the most stressing because it gives the largest tilt of the photon sieve. In addition to the in- and out-of-plane deformations, we also determined the tip/tilt and decentering of the photon sieve due to these misalignments and found that these displacements have the greatest effect on the imaging performance of the telescope.

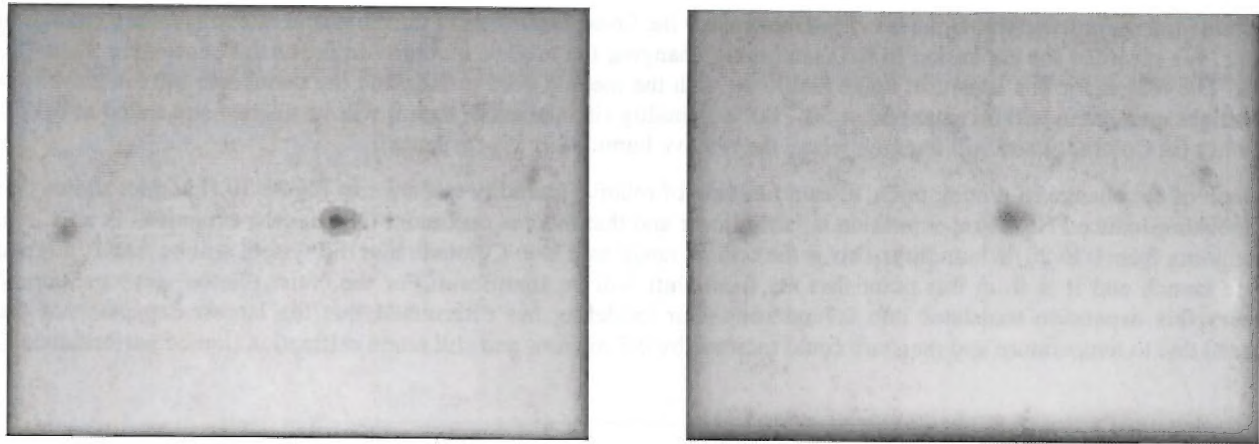


Figure 8. Imaging of the Sun (modeled by Zemax) if deployment is ideal (left) and if the tips of the de-coupling springs are misaligned and the photon sieve is not properly positioned (right).

The RMS wavefront error of the deformed photon sieve surface in the nominal (ideal) case is 0.063 waves and the image is diffraction limited. In the off nominal case surface deformations lead to performance that is 13 times worse than the diffraction limit, mostly due to decenter and tilt of the photon sieve relative to the optical axis.

4.4 Thermal and humidity expansion of the membrane material

The optimal focusing capability of the photon sieve depends on the holes being located according to precise design tolerances⁹. Ideally it would be preferable to have the hole positions controlled to within a tenth of the underlying zone width which for an $f/2$ primary translates into a CTE of the order of $10^{-7} / ^\circ\text{C}$. We measured the CTE of a 2cm x 10 cm piece of membrane material (Novastrat) patterned with a diffraction grating. A photodiode was arranged to view a small point on the fringe pattern created by the interference of the first and zero order diffracted beams. As the temperature of the film was varied the grating expands and contracts, changing the angle of diffraction of the first order, which is reflected in motion of the fringes over the photodiode. Careful monitoring of the fringe shift with temperature thus correlates to the thermal expansion. A graph of the shift in d as a function of temperature is shown in Fig. 9 and from this we determined the average CTE to be $6.3 \times 10^{-7} (/ ^\circ\text{C})$. From this we can expect a maximum expansion of around 5 microns at the edge of the 0.2m diameter sieve under the expected 80°C temperature swing in LEO.

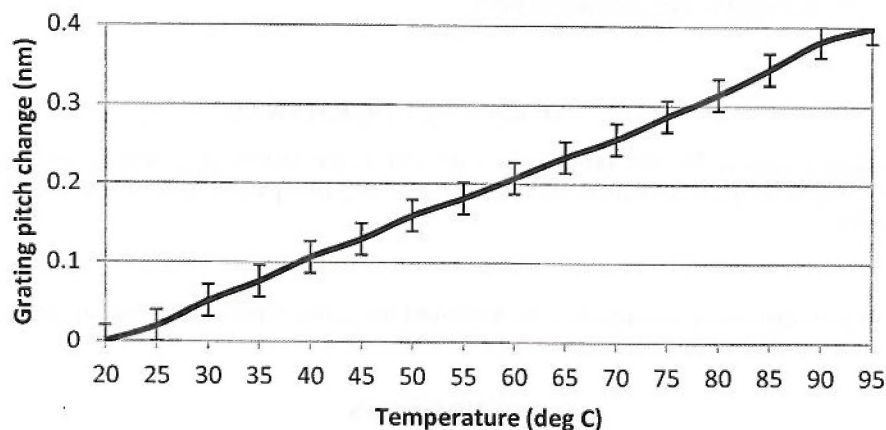


Figure 9. Change in grating pitch as a function of temperature.

The same interferometric technique was used to measure the linear expansion of the Novastrat due to moisture content in the air. We recorded the expansion in the material by changing the relative humidity in the airtight enclosure from 8 to 91 %. The reason for this large test range had to do with the method used to fabricate the membrane photon sieve: our final flight membrane will be patterned at 50 – 80 % humidity (in Alabama), then it will be aligned and tested at 6-17% humidity (in Colorado) and will imaging where the relative humidity is 0% (in space).

A graph of the change in grating pitch, d , as a function of relative humidity is shown in Figure 10. The plot shows that the moisture-induced Novastrat expansion is fairly linear and that there is maximum 0.07 micron expansion in a 2x2 cm piece going from 0 to 20 % humidity. This is the critical range as it is in Colorado that the system will be finally aligned before launch and it is from this point that the focal shift will be significant. For the entire photon sieve membrane primary this expansion translates into 0.7 microns. Our modeling has determined that the largest expansion of the material due to temperature and moisture could increase by 0.7 microns and still retain diffraction limited performance.

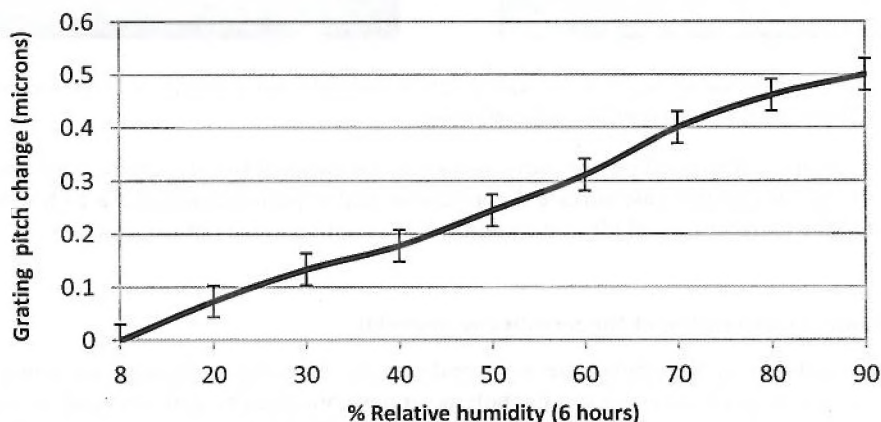


Figure 10. The change in grating pitch as a function of relative humidity.

5. CONCLUSION

We have completed the design and testing of a 0.2 m photon sieve master for the FalconSAT-7 telescope, which will be used to manufacture a stowed membrane primary. There are two main factors that may contribute to image quality: environmental changes and deployment precision. CTE and CHE measurements confirm that so far Novastrat polyimide is a suitable material to use in orbit. An opto-mechanical analysis of the deployment structure that supports the membrane photon sieve showed that in the worst deployment case the RMS wavefront error will be 0.95 waves and the image quality will be 13 times worse than diffraction limit.

6. ACKNOWLEDGEMENTS

We wish to acknowledge support for this project from the Air Force Office of Scientific Research (AFOSR). The construction of this satellite is a collaborative effort that includes participation from HUA Inc., MMA Design Inc., NASA, AFIT and AFRL.

Distribution Statement: Distribution A, Approved for public release, distribution unlimited.

REFERENCES

- [1] Andersen, G. "Membrane photon sieve telescopes," *Appl. Opt.* **49**, 6391-6394 (2010).
- [2] Kipp, L., Skibowski, M., Johnson, R. L., Berndt, R., Adelung, R., Harm, S., and Seemann, R., "Sharper images by focusing soft X-rays with photon sieves," *Nature* **414**, 184-188 (2001).

- [3] Andersen, G., Asmolova, O., Dearborn, M., McHarg, M., "FalconSAT-7: A membrane photon sieve CubeSat Solar Telescope," Proc. SPIE **8442**, 84421C (2012).
- [4] Xie, C., Zhu, X., Jia, J., "Focusing properties of hard x-ray photon sieves: three-parameter apodization window and waveguide effect," Opt. Lett. **34**, 3038-3040 (2009).
- [5] Andersen, G., "Large optical photon sieve," Opt. Lett. **30**, 2976-2978 (2005).
- [6] Andersen, G., and Tullson, D., "Broadband antihole photon sieve telescope," Appl. Opt. **46**, 3706-3708 (2007).
- [7] Zhou, C., Dong, X., Shi, L., Wang, C., Du, C., "Experimental study of a multiwavelength photon sieve designed by random-area-divided approach," Applied optics, Vol. 48, No. 8, 1619-1623 (2009).
- [8] K. Doyle, V. Genberg, G. Michels, G. Bisson, "Optical modeling of finite element surface displacements using commercial software", Proc. SPIE, **5867**, 18 (2005).
- [9] Zhang, J., Cao, Q., Lu, X., Lin Z., "Focusing contribution of individual pinholes of a photon sieve: dependence on the order of local ring of underlying traditional Fresnel zone plate," Chinese Opt. Lett., **8**, 256-258 (2010).

